Bulletin of Earthquake Engineering (2023) 21:1627–1650
https://doi.org/10.1007/s10518-022-01378-z

S.I. : ADVANCES ON INERTER-BASED SEISMIC PROTECTION OF STRUCTURES

Mitigating jacket offshore platform vibration under earthquake and ocean waves utilizing tuned inerter damper

Tiancheng Xu[1] · **Yancheng Li**[1,2] · **Dingxin Leng**[3]

Received: 16 August 2021 / Accepted: 28 February 2022 / Published online: 26 March 2022

Abstract
The unwanted vibrations of offshore structures induced by wave or earthquake loads can lead to the reduction of the service life and fatigue failure of the offshore platforms. This paper introduces tuned inerter damper (TID) to a jacket offshore platform as passive control device for mitigating the excessive vibrations of platform structure induced by wave and earthquake loads. An analytical design method is proposed for jacket platforms and the influence of installation location on the modal response is investigated. The proposed design method can determine the optimal installation position and obtain the optimal design parameters by transform the original multi-degree of freedom (MDOF) system to a single DOF (SDOF) modal system. Two sets of closed-form solutions of which corresponding to wave and earthquake excitations are derived based on the H_2 optimization criterion. Further, a practical 90 (m) high and 80 (m) deep in-water jacket offshore platform is used in numerical simulation and the wave forces are modeled using Morison's equation. The case study finds that the optimal installation location of TID is deck level for both wave and earthquake loads. The proposed design method is validated by the numerical example and the results demonstrate that TID system can effectively mitigate the maximum, minimum, and RMS responses of jacket platforms. Besides, the TID is more effective when the jacket platform is under the action of waves and the tuning of TID according to earthquake load is more reliable when the jacket platform subjected to both wave and seismic loads.

Keywords Tuned inerter damper · Jacket offshore platform · Vibration mitigation · Earthquake · Oceanwave

✉ Yancheng Li
yli@njtech.edu.cn; yancheng.li@uts.edu.au

[1] College of Civil Engineering, Nanjing Tech University, Nanjing 211816, China

[2] School of Civil and Environmental Engineering, University of Technology Sydney, Ultimo, NSW 2007, Australia

[3] Department of Mechanical and Electrical Engineering, Ocean University of China, Qingdao, Shandong, China

1 Introduction

Jacket offshore platforms are the most widely used offshore platforms and are extensively used for exploration, production and storage of ocean resources. The jacket offshore platforms inevitably experience unwanted vibrations induced by ocean excitations, including winds, currents, waves, ice and sometimes earthquakes loadings (Hirdaris et al. 2014). These actions of excitation loadings may affect functionalities of the structures and lead to fatigue failure of structures, discomfort of person and even severe structural damage (Zhang et al. 2017). Among those ocean excitations, waves and earthquake are two main loads in the design of offshore structures if an offshore platform is located in a seismically active region. As such, the jacket offshore platforms will interact with the water pounding and the ground motion, which possess distinct frequency features and hence impose great challenge. Thus it is important to analyze the dynamic responses of jacket offshore platforms under waves and earthquake loads and it is of great significance to protect offshore platforms from natural hazard, especially under extreme case when two extreme events occur at the same time.

A widely utilized way to suppress the unwanted vibrations or damage of offshore platforms is the structural control approach including passive (Lee 1997), semi-active control (Leng et al. 2021), active control, and hybrid control. The passive control schemes, including passive energy dissipation mechanisms, damping isolation mechanisms, and dynamic vibration absorbers (DVA), have been used extensively for jacket offshore structures in the last two decades due to excellent vibration control performance and high stability, low cost and minimal-to-none requirement on external power. Passive energy dissipation devices include hysteretic and viscoelastic dampers are used for jacket offshore platforms extensively. Patil and Jangid (2005) studied the wave-induced response of an offshore jacket platforms with various energy dissipation devices such as viscoelastic and viscous and friction dampers. It is observed that passive energy dissipation dampers are effective to reduce response of jacket platform structures and the viscoelastic dampers outperform the other dampers. Vaezi et al. (2020, 2021) investigated the application of brace-viscous damper in mitigation of dynamic response of a jacket platform and the effects of different configurations (toggle, chevron, and diagonal) and brace stiffness of brace-viscous damper on control performance. Besides, new type dampers like the shape memory alloy (SMA) (Enferadi et al. 2019) is adopted to mitigate responses of jacket offshore platforms subjected to wind loading. Damping isolation mechanism, which is proposed to implement between the bottom of deck and above the jacket structure, is another approach that can reduce and dissipate the unwanted response of offshore platforms. A damping isolation system composed of rubber bearings and viscous dampers is developed for vibration mitigation of a real jacket offshore platform subjected to earthquake and ice loads (Ou et al. 2007). In Liu et al. (2009), an acceleration-oriented optimization design approach for ice-resistant jacket offshore platform is proposed and the study reveals the acceleration response of deck dominates the occupant comfort and fatigue life of platform structure. DVAs, represented by tuned mass dampers (TMDs) and tuned liquid dampers (TLDs), have been extensively used to control the responses of jacket offshore platforms. A TMD device is composed of a mass in series to a parallel connection of a spring and a dashpot. TMDs are extensively used for jacket offshore platforms to suppress response of target vibration mode of primary structure due to obvious advantages in cost-effectiveness. In Yue et al. (2009), a TMD device is used to mitigate ice-induced vibrations of jacket platform. Pourzangbar and Vaezi (2021) design the brace-viscous damper system and pendulum tuned mass damper system by

particle swarm optimization to mitigate unwanted response of a jacket platform subjected to wave loading. In addition, many researchers also examined the TLD devices (Chaiviriyawong et al. 2007; Jin et al. 2007), the semi-active control (Bin et al. 2011), and the active control (Suhardjo and Kareem 2001) for vibration control of jacket offshore platforms.

Recently, a new mechanical device called inerter is introduced into passive control to combine with conventional passive control elements for their performance improvement (Ma et al. 2021). Inerter, invented by Smith (2002), is a two-terminal device, and the two terminals can produce force proportional to the difference of acceleration of two terminals and the proportional coefficient is called inertance or apparent mass with the unit of mass. A common configuration of inerter includes a flywheel, a rack, and gears. The distinguished advantage of inerter is that a considerable inertance, which can be hundreds of times higher than the actual mass of flywheel, can be achieved through the rack mechanism and, thereby, inerter-based system can achieve excellent control performance with low mass cost. Up to date, considerable efforts have been devoted to application of inerter-based systems in mitigation of unwanted responses in civil engineering structures. Tuned viscous mass damper (TVMD) is a seismic control system based on inerter proposed by Ikago et al. (2011) for civil buildings and the effectiveness of TVMD for vibration control is verified by shake table tests with a small-scale TVMD (Ikago et al. 2012). Marian and Giaralis (2014) proposed tuned mass damper inerter (TMDI), which adds an inerter to the classical TMD, to enhance the vibration control performance of TMD. The optimal design and evaluation of TMDI for seismic excitations is analytically investigated (Pietrosanti et al. 2017) and the application of TMDI for mitigating vibration of tall buildings induced by wind is studied in Giaralis and Petrini (2017). The TMDI is also used to suppress the excessive vibration induced by vortex for bridges (Xu et al. 2019; Angelis et al. 2021) and to enhance the performance of base isolation systems by coupled the systems with a TMDI (Domenico and Ricciardi 2018a, b; Matteo et al. 2019; Angelis et al. 2019).

Tuned inerter damper (TID) which substituting the mass element of TMD by the inerter, proposed by Lazar et al. (2014), is another promising inerter-based passive control system and is regarded as an attractive alternative to TMD. A numerical search approach based on fixed point method is proposed by Lazar et al. to find the optimal parameters of TID for ground motion excitation and it is analytically seen that the optimal installation location of TID is at the bottom floor of buildings. Hu et al. (2015) and Hu and Chen (2015) examined the H_2 and H_∞ optimization problem of various inerter-based control systems and the analytical solutions of inerter-based control systems are derived for undamped primary structures. Gonzalez-Buelga et al. (2017) investigate the effect of inerter nonlinearities on the performance of TID by a hybrid experimental test. TID is also used to suppress the vibration of cables in cable-stayed bridges induced by wind or earthquake and the numerical results show that TID has superior control performance over traditional passive control systems like viscous dampers (VD) and TMD (Lazar et al. 2016; Sun et al. 2017). Shen et al. (2019) examined the seismic control performance of TID and analytical formulas of optimal parameters of TID for undamped structures considering different target response are derived. In Xu et al. (2021, 2022) proposed a simplified design approach to obtain the analytical formulas of TID for damped MDOF structures utilized the equivalent linearization method and the optimal position of TID for earthquake excited buildings is analytically determined as in the bottom floor.

Recently, the inerter-based devices have been applied to offshore structures. Hu et al. (2018), different inerter-based passive control devices are used for a barge-type floating offshore wind turbine to suppress the responses induced by wind and wave and the effect of inerter-based devices is demonstrated. In Ma et al. (2018), a new inerter-based

control system called tuned heave plate inerter (THPI) is proposed to mitigate the excessive vibration of semi-submersible platforms (SSP) subjected to wave loading and the analysis shows the proposed THPI has better control effect than conventional tuned heave plate. Further, Ma et al. (2019) proposed another inerter-based system called rotational inertia damper (RID) for the control of heave motion of SSP located in shallow sea and the results demonstrated that excellent control effectiveness can be achieved with low mass cost. Based on the previous studies, Ma et al. (2020) further improve the ability of RID such that not only the heave motion but also the pitch motion of SSP can be controlled. To sum up, there is still limited studies on the application of inerter-based control system for offshore platforms, especially for the common used jacket platforms. Besides, to the best of the authors' knowledge, the design and evaluation of inerter-based system for offshore platforms subjected to earthquake load or both the earthquake and wave load have not been reported in literatures. Therefore, it is of great signification to investigate the fundamental mechanism and control performance of inerter-based device for jacket offshore platforms considering wave and earthquake loads.

In the present study, a representative inerter-based passive control system-TID device is used to control dynamic response of a real jacket offshore platform subjected to wave and earthquake loads. In Sect. 2.1 a theoretical model is introduced to represent jacket offshore platform with TID device, considering both wave and earthquake loads. Then in Sect. 2.2 the optimal installed location of TID is determined through modal analysis and in Sect. 2.3 two sets of closed-form solutions which can obtain the optimal design parameters of TID is proposed for wave and earthquake loads, respectively. In Sect. 3 a numerical example is presented considering a real jacket offshore platform controlled by TID to verify the proposed design method and the effectiveness of the TID. Finally, the dynamic responses of the offshore structure-TID system subjected to wave and earthquake loads are evaluated and compared.

2 Theoretical analysis

2.1 Theoretical model

In Fig. 1, a jacket offshore platform is modeled as an n degrees of freedom (DOF) lumped mass model. The TID is installed at adjacent levels $i-1$ and i of offshore platform and the installation location of TID is called ith level at this moment for convenience. Note $i \in [1, n]$ and when $i = 1$ it means the TID is installed between first level and the base. m_i, c_i, and k_i are the lumped mass, damping, and lateral stiffness coefficients of ith level of platform respectively; b, c_d, and k_d are the inertance, damping, and stiffness coefficients of TID, respectively. y_i is the relative displacement of the ith level relative to the base. a_g is the base acceleration with the frequency ω and f_{wi} is the wave loadings at ith level.

The equations of motions of the jacket offshore platform-TID system is written as follows,

$$[\mathrm{M}]\{\ddot{y}(t)\} + [\mathrm{C}]\{\dot{y}(t)\} + [\mathrm{K}]\{y(t)\} = \{p\} + \left\{f_{\mathrm{TID}}\right\} \tag{1}$$

where

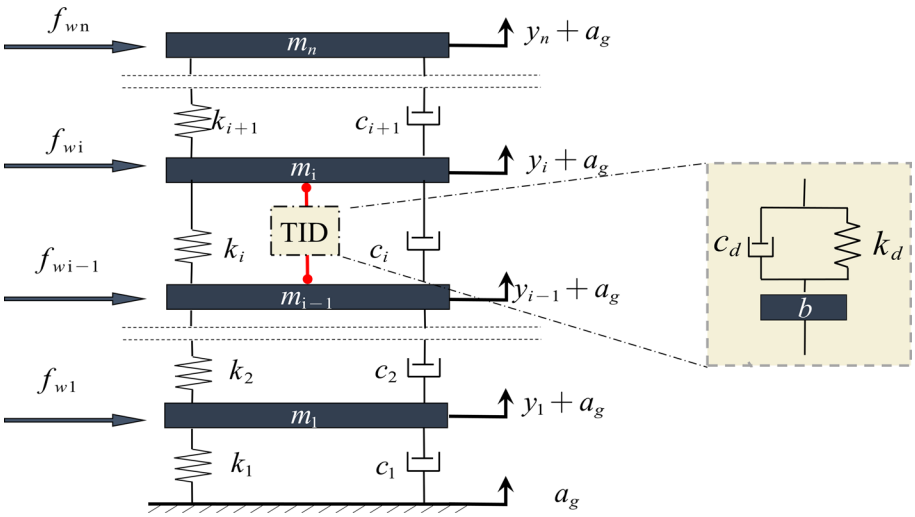

Fig. 1 Analysis model of a n-DOF jacket offshore platform controlled by a TID system

$$\{p\} = \begin{cases} -\{m_1, m_2, ..., m_n\}^{\mathrm{T}} a_g, Case\,I: for\ base\ (\text{earthquake})\ excitation \\ \{f_w\}, Case\,II: for\ irregular\ wave\ exciation \end{cases} \tag{2}$$

and $[\mathrm{M}] \in \mathbf{R}^{N\times N}, [\mathrm{C}] \in \mathbf{R}^{N\times N}, [\mathrm{K}] \in \mathbf{R}^{N\times N}$ are the mass, damping and stiffness matrices of the platform structure, respectively; $\{\ddot{y}(t)\}, \{\dot{y}(t)\}and\{y(t)\}$ are the relative acceleration, velocity, and displacement response vectors, respectively; $\{p\}$ is the excitation force vector which has two cases: case I is the earthquake excitation and case II is the wave excitation. $\{f_w\}$ is the wave loading force vector; $\{f_{\mathrm{TID}}\}$ is control force vector produced by TID. The superscript T denotes the transpose of matrix. The matrices and vectors in Eq. (1) can be developed as in

$$[\mathrm{M}]\{\ddot{y}(t)\} = \begin{bmatrix} m_1 & & & \\ & m_2 & & \\ & & \ddots & \\ & & & m_n \end{bmatrix} \begin{bmatrix} \ddot{y}_1(t) \\ \ddot{y}_2(t) \\ \vdots \\ \ddot{y}_n(t) \end{bmatrix}, [\mathrm{K}]\{y(t)\} = \begin{bmatrix} k_1 + k_2 & -k_2 & & \\ k_2 & k_2 + k_3 & & \\ & & \ddots & \\ & & & k_n \end{bmatrix} \begin{bmatrix} y_1(t) \\ y_2(t) \\ \vdots \\ y_n(t) \end{bmatrix} \tag{3}$$

$$[\mathrm{C}]\{\dot{y}(t)\} = \left(\alpha_0[M] + \alpha_1[K]\right) \begin{bmatrix} \dot{y}_1(t) \\ \dot{y}_2(t) \\ \vdots \\ \dot{y}_n(t) \end{bmatrix} \tag{4}$$

$$\{f_w\} = \left(f_{w1}, f_{w2}, ..., f_{wn}\right)^{\mathrm{T}} \tag{5}$$

$$\{f_{\mathrm{TID}}\} = \{L\} f_{\mathrm{TID}} \tag{6}$$

At presented in Eq. (4), the damping matrix of platform system is considered as Rayleigh damping with the Rayleigh constants α_0 and α_1. The damping ratio will be considered as 0.02 in following case study.

In Eq. (6), f_{TID} is the control force produced by the TID system; $\{L\} \in \mathbf{R}^{N\times 1}$ is the installation location vector defined as follows

$$\{L\} = \begin{cases} (0, ..., -1, 1, ..., 0)^{\mathrm{T}}, when i \neq 1 \\ (1, 0, ..., 0)^{\mathrm{T}}, when\ i = 1 \end{cases} \tag{7}$$

where (i−1)th entry and the ith entry of $\{L\}$ is -1 and 1, respectively, and the other entries are all 0. For the special case when TID is installed on 1st level, only the 1st entry is 1, and other entries are all zero.

Noting when consider the earthquake excitation, the system is identical with that for civil building in Xu et al. (2021), thus the previous works can be used here straightway. The analysis below will focus on the system subjected to irregular wave excitation.

2.2 Selection of optimal location of TID by modal analysis

Considering $\{p\} = \{f_w\}$ and zero initial conditions, the equations of motion Eq. (1) can be rewritten in Laplace domain as follows

$$\left([\mathrm{M}]s^2 + [\mathrm{C}]s + [\mathrm{K}]\right)\{Y\} = \{F_w\} + \{L\}F_{\mathrm{TID}} \tag{8}$$

where $\{Y\} = \mathcal{L}(\{y(t)\}) = \left(Y_1, Y_2, \cdots, Y_n\right)^{\mathrm{T}}$ and $\mathcal{L}(\cdot)$ is Laplace transform operator; s is the Laplace variables and $\{F_w\} = \mathcal{L}(\{f_w\})$.

$F_{\mathrm{TID}} = \mathcal{L}\left(f_{\mathrm{TID}}\right)$ is the control force produced by TID and it is

$$F_{\mathrm{TID}} = -\frac{s}{\frac{1}{k_d/s} + \frac{1}{bs}}\{L\}^{\mathrm{T}}\{Y\} \tag{9}$$

Then consider the transformation $\{Y\} = [\Phi]\{Q\}$, where $[\Phi]$ is the modal matrix as follows

$$[\Phi] = \left[\{\phi_1\}, \{\phi_2\}, ..., \{\phi_n\}\right] = \begin{bmatrix} \phi_{1,1} & \phi_{1,2} & \cdots & \phi_{1,n} \\ \phi_{2,1} & \phi_{2,2} & \cdots & \phi_{2,n} \\ \vdots & \vdots & \ddots & \vdots \\ \phi_{n,1} & \phi_{n,2} & \cdots & \phi_{n,n} \end{bmatrix}$$

and $\{Q\}^T = \{q_1, q_2, ..., q_n\}$ denotes the generalized coordinates. In general, $\{Y\}$ is obtained by superposing all the generalized coordinates, i.e. $\{Y\} = \{\phi_1\}q_1 + \{\phi_2\}q_2 + \cdots + \{\phi_n\}q_n$. If the TID is to be designed for jth mode, it is reasonable to assume only the jth modal response is dominated and there is no significant modal interaction, which leads to $\{Y\} \approx \{\phi_j\}q_j$. If [C] is a proportional damping matrix, substituting $\{Y\} \approx \{\phi_j\}q_j$ into Eq. (8) and pre-multiplying both sides by $\{\phi_j\}^{\mathrm{T}}$, one obtains

$$\tilde{m}_j q_j s^2 + \tilde{c}_j q_j s + \tilde{k}_j q_j = \{\phi_j\}^{\mathrm{T}}\{F_w\} - s\left(\frac{1}{k_d/s} + \frac{1}{bs}\right)^{-1}(\phi_{i,j} - \phi_{i-1,j})^2 q_j \tag{10}$$

where $\tilde{m}_j = \{\phi_j\}^{\mathrm{T}}[\mathbf{M}]\{\phi_j\}, \tilde{c}_j = \{\phi_j\}^{\mathrm{T}}[\mathbf{C}]\{\phi_j\}$, and $\tilde{k}_j = \{\phi_j\}^{\mathrm{T}}[\mathbf{K}]\{\phi_j\}$ are the modal mass, damping, and stiffness, respectively. From Eq. (10) a transform function from $\{\phi_j\}^{\mathrm{T}}\{F_w\}$ to q_j can be obtain

$$\frac{q_j}{\{\phi_j\}^{\mathrm{T}}\{F_w\}} = \frac{1}{\tilde{m}_j s^2 + \tilde{c}_j s + \tilde{k}_j + s\left(\frac{1}{k_d/s} + \frac{1}{bs}\right)^{-1}(\phi_{i,j} - \phi_{i-1,j})^2} \tag{11}$$

From above equation it can be seen that the modal response is dependent on the installation location of TID. A larger value of $(\phi_{i,j} - \phi_{i-1,j})^2$ will reduce the value of q_j, and vice versa. Thus the optimal installation location of TID is ith level which can maximize the $(\phi_{i,j} - \phi_{i-1,j})^2$. In other words, the level whose drift is maximum in jth modal shape is the optimal location of TID when targeting jth modal of offshore platform for control. This conclusion is the same with that when the excitation is earthquake (Xu et al. 2021). Therefore, the optimal installation location of TID for jacket offshore platform is the same whether the excitation is wave loading or earthquake loading.

2.3 Tuning of the TID system

The most important aspect in design of passive control device is the choice of optimal parameters for excellent control performance. For design of TID, the inertance b is fixed while the damping c_d and stiffness k_d need to be tuned. The optimal c_d and k_d of TID when targeting jth mode will be determined analytically by a method followed here.

The concept of the method is to transform the original matrix equation to scalar modal equations. The analysis can proceed by a transformation of coordinates. Noting in $\{Y\} \approx \{\phi_j\}q_j$, there have

$$Y_i \approx \phi_{i,j} \times q_j \tag{12}$$

and

$$Y_{i-1} \approx \phi_{i-1,j} \times q_j \tag{13}$$

Let Eq. (12) minus Eq. (13), one obtains

$$Y_i - Y_{i-1} \approx (\phi_{i,j} - \phi_{i-1,j}) \times q_j \tag{14}$$

For convenience, the approximately equals sign is replaced by the equals sign and solving for q_j

$$q_j = \frac{Y_i - Y_{i-1}}{\phi_{i,j} - \phi_{i-1,j}} \tag{15}$$

and then substituting in Eq. (10), one obtains

$$\frac{\tilde{m}_j(Y_i - Y_{i-1})s^2}{(\phi_{i,j} - \phi_{i-1,j})^2} + \frac{\tilde{c}_j(Y_i - Y_{i-1})s}{(\phi_{i,j} - \phi_{i-1,j})^2} + \frac{\tilde{k}_j(Y_i - Y_{i-1})}{(\phi_{i,j} - \phi_{i-1,j})^2} = \frac{\{\phi_j\}^T\{F_w\}}{\phi_{i,j} - \phi_{i-1,j}} - s\left(\frac{1}{k_d/s} + \frac{1}{bs}\right)^{-1}(Y_i - Y_{i-1}) \tag{16}$$

Taking

$$m_{je} = \frac{\tilde{m}_j}{(\phi_{i,j} - \phi_{i-1,j})^2}, c_{je} = \frac{\tilde{c}_j}{(\phi_{i,j} - \phi_{i-1,j})^2}, k_{je} = \frac{\tilde{k}_j}{(\phi_{i,j} - \phi_{i-1,j})^2}, F_{wje} = \frac{\{\phi_j\}^T\{F_w\}}{\phi_{i,j} - \phi_{i-1,j}} \tag{17}$$

transform the modal equations Eq. (16) to an equivalent SDOF system equations as

$$m_{je}\left(Y_i - Y_{i-1}\right)s^2 + c_{je}\left(Y_i - Y_{i-1}\right)s + k_{je}\left(Y_i - Y_{i-1}\right) = F_{wje} - s\left(\frac{1}{k_d/s} + \frac{1}{bs}\right)^{-1}\left(Y_i - Y_{i-1}\right) \tag{18}$$

where m_{je}, c_{je}, k_{je}, andF_{we} denote the equivalent mass, damping, stiffness, and wave loading parameters of the equivalent SDOF system. The response of the system is $Y_i - Y_{i-1}$ and the transform function from F_{wje} to $Y_i - Y_{i-1}$ is

$$\frac{Y_i - Y_{i-1}}{F_{wje}} = \frac{1}{m_{je}s^2 + c_{je}s + k_{je} + s\left(\frac{1}{k_d/s} + \frac{1}{bs}\right)^{-1}} \tag{19}$$

Meanwhile, several dimensionless parameters are introduced as

$$\mu = \frac{b}{m_{je}}, \gamma = \frac{\omega_d}{\omega_j}, \xi_d = \frac{c_d}{2b\omega_d}, \xi_s = \frac{c_{je}}{2m_{je}\omega_j} \tag{20}$$

where μ denotes the inertance-equivalent mass ratio; γ is the tuning ratio (or frequency ratio); ξ_d and ξ_s are the damping ratios of TID system and offshore platform structure, respectively; And

$$\omega_d = \sqrt{\frac{k_d}{b}}, \omega_j = \sqrt{\frac{k_{je}}{m_{je}}} = \sqrt{\frac{\tilde{k}_j}{\tilde{m}_j}}$$

are the natural frequencies of TID and offshore platform, respectively.

When the system is subjected to random loadings such as the wave, flow current or earthquake process, the H_2 optimization criterion is suitable for passive control devices. In the H_2 optimization, the aim is to minimize the total energy of responses or the mean square responses of the system subjected to a Gaussian white noise excitation, i.e., the power spectral density is same for all frequency and here a constant S_0 can be used to represent the spectral density. Generally, the analytical solutions of TID for H_2 optimization exist if the primary is undamped and will be derived as follows. The performance index to be minimized of H_2 optimization is defined as

$$J = \frac{E\left[\left(Y_i - Y_{i-1}\right)^2\right]}{2\pi S_0\omega_j} \tag{21}$$

where $E\left[\left(Y_i - Y_{i-1}\right)^2\right]$ is the mean square value of the responses of the equivalent SDOF system, it can be calculated by

$$E\left[\left(Y_i - Y_{i-1}\right)^2\right] = S_0\int_{-\infty}^{\infty}|H(\mathbb{i}\omega)|^2 d\omega = S_0\omega_j\int_{-\infty}^{\infty}|H(\lambda)|^2 d\lambda \tag{22}$$

where $\lambda = \omega/\omega_j$ is the frequency ratio; $\mathbb{i} = \sqrt{-1}$ is the imaginary unit; and

$$H(\lambda) = \frac{Y_i - Y_{i-1}}{F_{wje}k_{je}} = \frac{\lambda^2 - \gamma^2 - 2\mathbb{i}\xi_d\lambda\gamma}{\begin{array}{l}\gamma^2 + \lambda^4 - \lambda^2\left((1+\mu)\gamma^2 + 4\xi_s\xi_d\gamma + 1\right) + \\ -2i\left(\xi_s + \xi_d\gamma + \xi_d\gamma\mu\right)\lambda^3 + 2\left(\xi_s\gamma^2 + \xi_d\gamma\right)\lambda\end{array}} \tag{23}$$

is the dimensionless transform function derived from Eq. (19). Substituting Eq. (22) into (21), then the performance index J can be rewritten as

$$J = \frac{1}{2\pi}\int_{-\infty}^{\infty} |H(\lambda)|^2 d\lambda \tag{24}$$

The performance index J can be calculated as

$$J = \frac{1}{4}\frac{n_1\xi_d^3 + n_2\xi_d^2 + n_3\xi_d + n_4}{d_1\xi_d^3 + d_2\xi_d^2 + d_3\xi_d + d_4}$$

$$\text{where}\begin{cases} n_1 = 4(1+\mu)\gamma^2 \\ n_2 = 4\gamma\left[(1+\mu)\gamma^2 + 1\right]\xi_s \\ n_3 = 1 + (1+\mu)^2\gamma^4 - \gamma^2\left(2 + \mu - 4\xi_s^2\right) \\ n_4 = \mu\gamma^3\xi_s \\ d_1 = -4\xi_s\gamma^2(\mu+1) \\ d_2 = \left(-4\xi_s^2\mu - 4\xi_s^2\right)\gamma^3 - \left(4\xi_s^2 + \mu\right)\gamma \\ d_3 = -\xi_s\left(\mu^2 + 2\mu + 1\right)\gamma^4 - \xi_s\left(4\xi_s^2 - 2\right)\gamma^2 - \xi_s \\ d_4 = -\xi_s^2\gamma^3\mu \end{cases} \tag{25}$$

Then the optimal parameters, according to Asami (Asami et al. 1991), can be found by the solution of partial differential equations:

$$\left.\begin{array}{l} \frac{\partial J}{\partial \gamma} = 0 \\ \frac{\partial J}{\partial \xi_d} = 0 \end{array}\right\} \tag{26}$$

After substituting Eq. (25) into Eq. (26), one obtains

$$\left.\begin{array}{l} 2\xi_d\xi_s(1+\mu)^2\gamma^5 + \left[3\xi_d^2(1+\mu)^2 + \xi_s^2\mu + 4\xi_d^2\xi_d^2(1+\mu)\right]\gamma^4 + \\ 2\gamma^3\xi_s\xi_d\left[4\xi_d^2(1+\mu) + \mu\right] + \xi_d^2\gamma^2\left[4\xi_d^2(1+\mu) - \mu - 2\right] - 2\gamma\xi_s\xi_d - \xi_d^2 = 0 \\ 4\gamma^2\xi_d^4(1+\mu) + 8\gamma^3\xi_s\xi_d^3(1+\mu) \\ +\left[4\xi_s^2\gamma^4(1+\mu) - 1 + \gamma^2(2+\mu) - \gamma^4(1+\mu)^2\right]\xi_d^2 - 2\mu\gamma^3\xi_s\xi_d - \mu\gamma^4\xi_s^2 = 0 \end{array}\right\} \tag{27}$$

The analytical solutions of Eq. (27) can be obtained if $\xi_s = 0$ and it is listed in Table 1. The optimal parameters of TID when the excitation is earthquake can be found in Xu et al. (2021) and also be listed below.

Finally, for given inertance b, the optimal damping c_d and stiffness k_d of TID system can be obtained by

Table 1 Optimal parameters of TID system for earthquake load (case I) and wave load (case II)

Case	load		Optimized index	Optimized parameters	
	Type	Applied to	J	γ	ξ_d
I	Acceleration	Frame	$\sqrt{\frac{(4-\mu)(\mu^2-\mu+1)}{4\mu}}$	$\sqrt{\frac{2-\mu}{2}}$	$\sqrt{\frac{\mu(\mu-4)}{8(\mu-2)(\mu^2-\mu+1)}}$
II	Force	Lumped mass	$\sqrt{\frac{4+3\mu}{4\mu(\mu+1)}}$	$\frac{\sqrt{2(\mu+2)}}{2(\mu+1)}$	$\sqrt{\frac{\mu(4+3\mu)}{8(1+\mu)(2+\mu)}}$

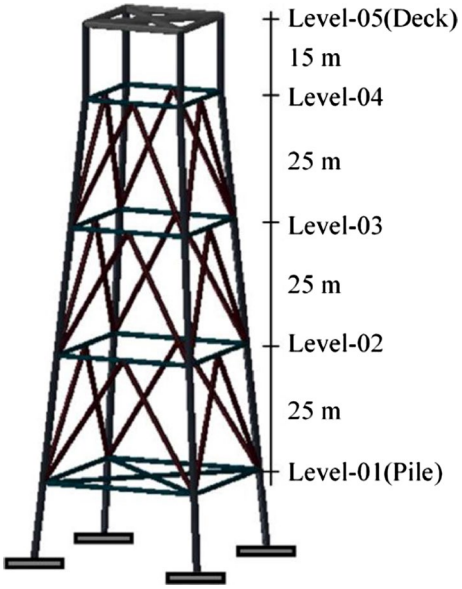

Fig. 2 Elevation view of the jacket platform (Ghasemi et al. 2019)

Table 2 Dynamic characteristics of the 5-level jacket platform

	Level-01	Level-02	Level-03	Level-04	Level-05
Mass (ton)	220	200	195	130	4850
Stiffness (KN/m)	90,000	350,000	210,000	115,000	42,000

$$\left.\begin{aligned} k_d &= b\gamma^2\omega_j^2 \\ c_d &= 2\xi_d\omega_j m_{je} \end{aligned}\right\} \tag{28}$$

3 Case studies and numerical analysis

In this section, the optimal design and performance evaluation of the TID on a realistic jacket offshore platform subjected to earthquake and wave excitations were evaluated. The response of the platform-TID systems were obtained considering different sea conditions and earthquake records.

A jacket offshore platform with representative characteristics has been selected as a case study (Ghasemi et al. 2019). The height of the platform is 90 (m) and the underwater part is 80 (m). For jacket, there have 4 legs with symmetrical dimensions $32 \times 32\left(\mathrm{m}^2\right)$ and $20 \times 20\left(\mathrm{m}^2\right)$ for sea floor and deck level, respectively. In each level of jacket, there has a steel inverted V-bracing is installed vertically. The elevation view of the platform is shown in Fig. 2.

The 5-level jacket platform is modeled as a 5-DOF system and the lumped mass and stiffness of each level are given in Table 2 (Enferadi et al. 2019). The natural frequencies

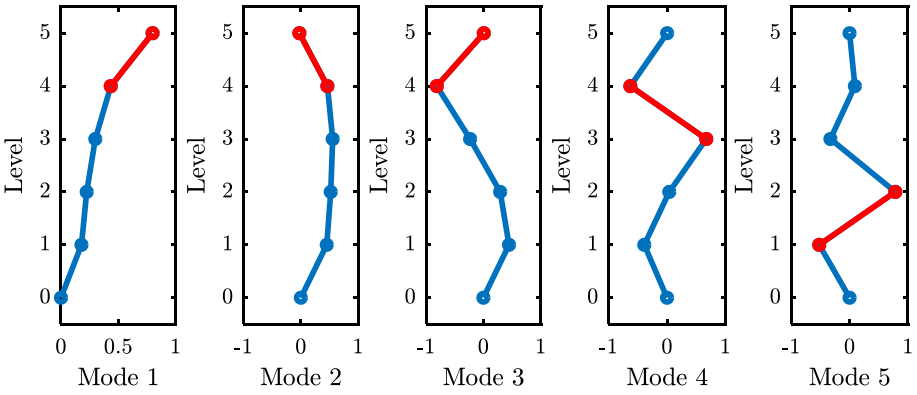

Fig. 3 vibration mode of jacket offshore platform and red lines are the maximal drift of each modal shape

Table 3 values of μ for mode 1 and considering different installation positions of TID

	Level-01	Level-02	Level-03	Level-04	Level-05
μ	0.0051	0.0003	0.0009	0.0029	0.0211

of the 1st to 5th modes are 1.98 rad/s, 12.83 rad/s, 30.96 rad/s, 46.43 rad/s and 66.34 rad/s, respectively.

The vibration mode of 5-DOF equivalent system of jacket offshore platform is shown in Fig. 3

As shown in Fig. 3, the maximal drift of mode 1, 2, and 3 all occur on top level. According to the proposed method, the optimal installation location of TID for jacket offshore platform when targeting low-order modes are top level. This result is different from that for civil buildings since the optimal position of TID for civil buildings, usually targeting first mode, is generally at the bottom level of building (Xu et al. 2021). This is because the mass of the deck, i.e. the top floor, is much larger than that of civil structure. Besides, for high-order modes, the optimal position of TID for jacket offshore platform is middle level and this is the same for civil buildings.

For jacket offshore platform, the first mode dominates the response. Thus the first mode is selected as the objective mode for control. Here chose inertance $b = 500$ton, which can be easily realized through the mass amplification ability of inerter. Then the μ considering each installation position of TID are calculated and listed in Table 3.

As shown in Table 3, μ is maximal when the position of TID is top level and is almost 4 times as large as that when TID is installed on bottom level. This result verifies the proposed method for the selection of optimal installation position of TID. Then the optimal parameters of TID can be obtained by substituting $\mu = 0.0211$ into Table 1 and Eq. (28).

3.1 Wave-induced loadings

To analyze the control performance of TID for the wave-induced vibration of the jacket offshore platform, the action of irregular waves reflecting the real sea conditions is important and is simulated. For obtained the irregular waves, JONSWAP wave spectrum and

the Morison equation are used to calculate the irregular waves with different dynamic characteristics.

In practical, the high degree of irregularity and randomness is required to represent the ocean waves. In case of an irregular wave, JONSWAP spectrum developed by Hasselmann et al. (1973) has gained wide acceptance to study the effect wave forces on the offshore structures (Das and Khan 2020; Hokmabady et al. 2019a, b). The JONSWAP wave spectrum is written as

$$S_{\eta}(\omega) = \alpha^* H_s^2 \frac{\omega_m^4}{\omega^5} \exp\left[-\frac{5}{4}\left(\frac{\omega_m}{\omega}\right)^4\right] \theta^{\exp\left[-\frac{(\omega-\omega_m)^2}{2\sigma^2\omega_m^2}\right]} \tag{29}$$

where α^* is the Goda coefficient (Goda 1970) and is determined by

$$\alpha^* = \frac{0.0624}{0.230 + 0.0336\theta - 0.185(1.9+\theta)^{-1}}; \tag{30}$$

ω_m is the spectral peak frequency; H_s is the significant wave height; θ is the peak enhancement factor. And σ is determined by

$$\begin{cases} \sigma = 0.07, & For\ \omega \le \omega_m \\ \sigma = 0.09, & For\ \omega > \omega_m \end{cases} \tag{31}$$

Utilizing the linear wave theory to calculate wave kinematics, the equations for the horizontal velocity and acceleration of fluid particle at location d can be given as follows,

$$\begin{cases} \dot{u}(t) = \sum_{x=1}^{h} \sqrt{2S(\widehat{\omega}_i)\Delta\omega_x}\omega_x \frac{\cosh(k_x d)}{\sinh(k_x z)} \cos(\widetilde{\omega}_x t + \varepsilon_x) \\ \ddot{u}(t) = -\sum_{x=1}^{h} \sqrt{2S(\widehat{\omega}_i)\Delta\omega_x}\omega_x^2 \frac{\cosh(k_x d)}{\sinh(k_x z)} \cos(\widetilde{\omega}_x t + \varepsilon_x) \end{cases} \tag{32}$$

in which $\widehat{\omega}_x = (\omega_{x-1} + \omega_x)/2$, $\widehat{\omega}_x$ represents the dominant frequency in x^{th} region; $\Delta\omega_x = (\omega_H - \omega_L)/M$, ω_H and ω_L are the maximum and minimum frequency in x^{th} region, respectively, and $M \in [50, 100]$; z represents the water depth; ε_x is a random value even distributed in the region of $[0 : 2\pi]$; k_x is the wave number.

Then the wave forces acting on the equivalent system of jacket offshore platform have been calculated by the Morison equation which expression is as follow:

$$f_w(z,t) = \frac{\pi}{4} C_M D^2 \rho \ddot{u}(z,t) + \frac{\rho}{2} C_D D |\dot{u}(z,t)| \dot{u}(z,t) \tag{33}$$

where $f_w(z,t)$ is the force acting on a unit length of a vertical cylindrical leg at a certain moment in which z is the water depth and t is time; C_M and C_D are the inertia and drag coefficients, as equal to 2 and 0.8, respectively; ρ is the seawater density which is 1030 kg/m^3; parameter D is the diameter of the vertical cylindrical leg of the jacket offshore platform (Table 4).

Table 4 Optimal parameters of TID for 5-DOF system considering earthquake load (case 1) and wave load (case II)

Case	γ (–)	ξ_d (–)	k_d (kN/m)	c_d (kNs/m)
I	0.9947	0.0735	1954.5	145.32
II	0.9845	0.0720	1914.6	140.86

Table 5 Dynamic characteristics of the irregular waves

Load case	Wave return period (year)	$T_p(s)$	$H_s(m)$
1	2	6.72	2.82
2	100	9.66	5.83

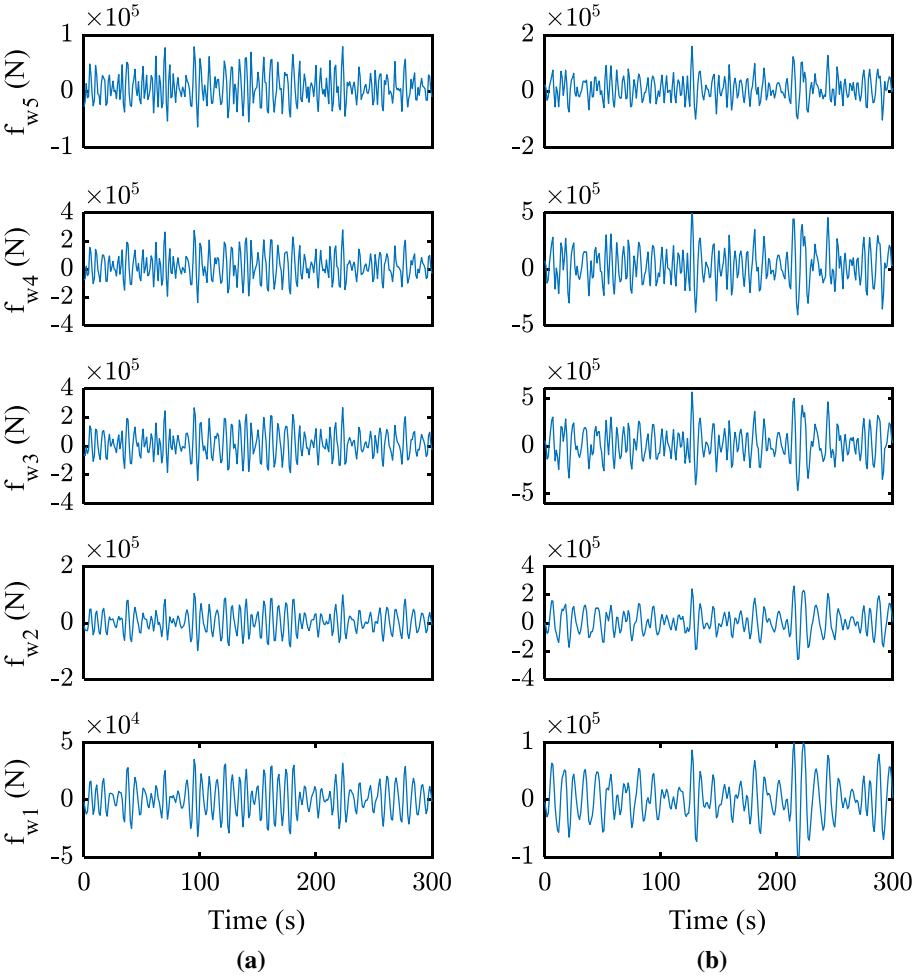

Fig. 4 Time history of irregular wave loads acting on the 5-DOF system platform: **a** load case 1 ($T_p = 6.72\,\text{s}, H_s = 2.82\,\text{m}$); **b** load case 2 ($T_p = 9.66\,\text{s}, H_s = 5.83\,\text{m}$)

Two load cases based on two irregular waves representing two different sea states are considered in the following numerical simulations. Dynamic characteristic

parameters of the two irregular waves are listed in Table 5 (Ghasemi et al. 2019), in which T_p is wave zero up crossing period.

The time history of irregular wave in terms of load case 1 and 2 are plotted in Fig. 4.

3.2 Earthquake loadings

Except for random sea wave load, the earthquake load is another important load for an offshore structure located in a seismically active region. Here four real earthquake excitation records are selected: El Centro, Hachinohe, Northridge, and Kobe earthquakes. The Takochi-oki (Hachinohe) earthquake, occurred on May 16, 1968 in the area offshore Aomori and Hokkaido in Japan at the depth of 26 km, is an offshore earthquake and is considered as representative in this paper. The seismic signal adopts north–south component at

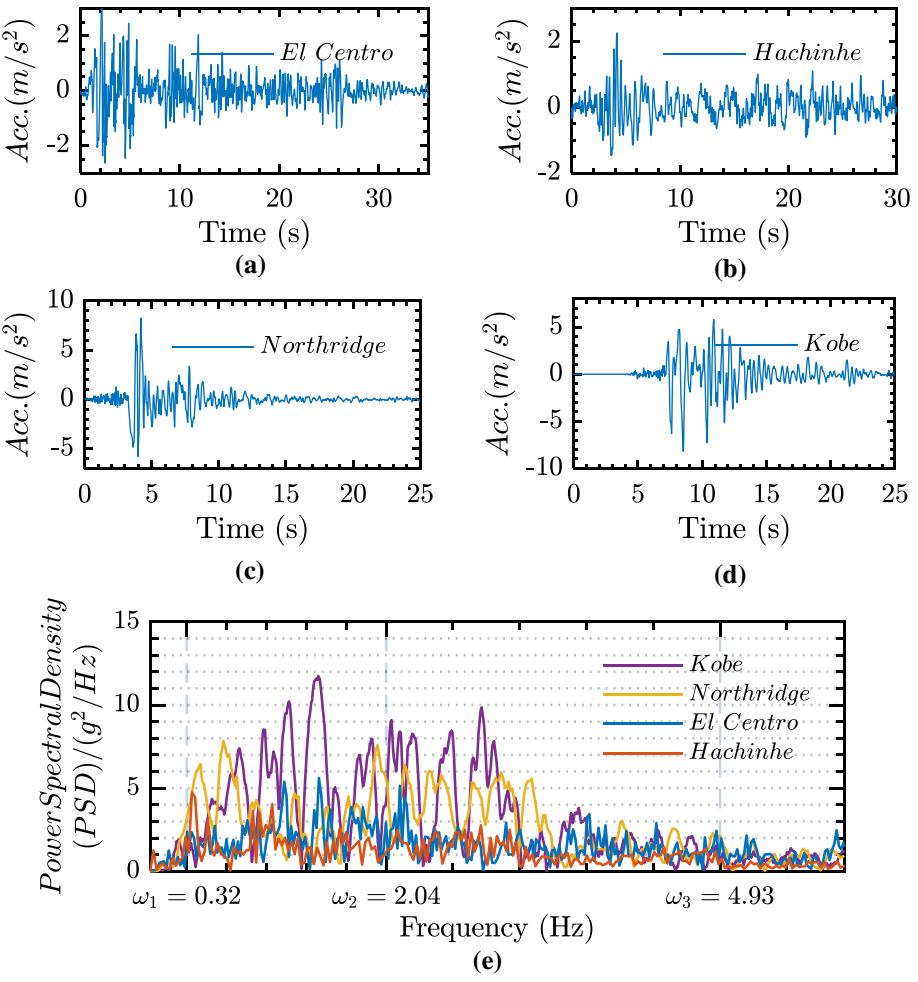

Fig. 5 Time history of **a** El Centro; **b** Hachinohe; **c** Northridge; **d** Kobe earthquakes; and **e** PSD of all the four earthquake signals

Hachinohe city during the Takochi-oki earthquake with the magnitude 7.9 and maximum acceleration 2.25 m/s^2. The time history and Power Spectral Density (PSD) of all the signals are shown in Fig. 5

From Fig. 5e, the range of frequency of all the four signals cover the first three natural frequencies of the platform structure. The PSD around ω_1 and ω_2 are dominant and the resonance can be triggered. It indicates TID can maximize the effect when installed on deck level.

3.3 Irregular wave response analysis

This section presents a numerical analysis to examine the control performance of TID system for jacket offshore platform. The dynamic responses of platform-TID system are evaluated for wave and earthquake ground motion inputs. Considering two load cases of wave, the dynamic responses of deck level of platform are shown in follows.

The time history deck displacements for two load case inputs are shown in Fig. 6. In the case of the 2-year period wave, the maximum deck displacement of jacket offshore platform without TID system controlled is 0.0359 m. Those are 0.0278 m and 0.0269 m for jacket offshore platform controlled by TID considered optimized TID in case I and II, respectively. The reduction ratios of case I and case II to uncontrolled case are 22.63% and 24.92%, respectively. In the case of the 100-year period wave, the maximum deck displacements of uncontrolled system and controlled system are 0.0792 m, 0.0497 m and 0.0484 m, respectively, and the reduction ratios are 37.20% and 38.92% for case I and II, respectively. The results verify the control effect of TID system on the wave-induced vibration of jacket

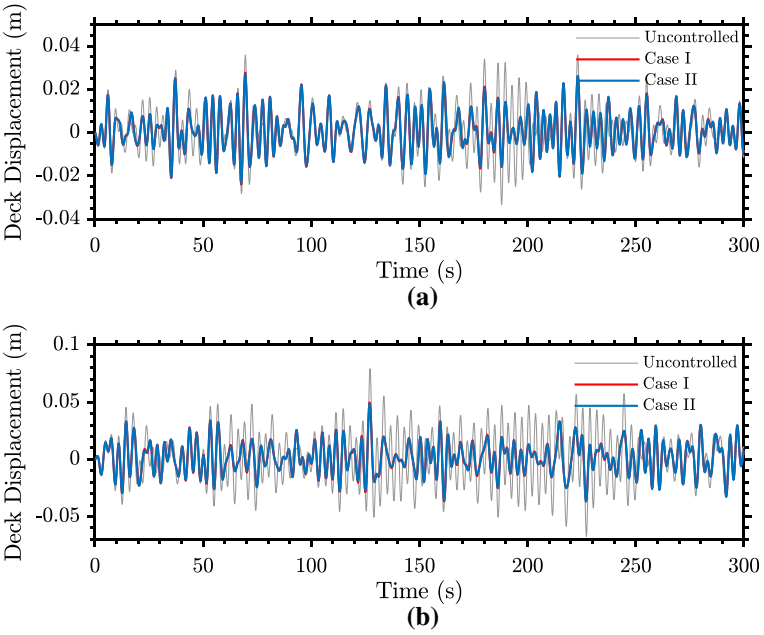

Fig. 6 Time history responses of jacket offshore platform deck displacement considering two optimization cases of TID system and two wave load cases: **a** load case 1, **b** load case 2

offshore platform and the TID performs better when the sea conditions are worse, i.e., 100-year period extreme wave. Note the μ of TID is only 0.0211 for mode 1 and it is entirely possible to increase further by inerter. Besides, the reduction ratio of case I and II are similar to each other but the effect of case II is slightly better than that of case I when system subjected to wave load. This indicates the design method for wave load is effective.

For acceleration responses case of deck level, the results are similar to that of displacement responses case, shown in Fig. 7. For the normal wave load, the maximum acceleration of deck of jacket offshore platform is reduced by 34.30% and 36.24% when the platform is controlled by TID in case I and II, respectively. While for the 100-year period wave, the reduction ratios are 43.71% and 44.78% for case I and II, respectively. The control effect of TID on acceleration response of jacket offshore platform is better than that of displacement response.

Besides max responses, minimum and root mean squares (RMS) responses of jacket offshore platform, with and without TID controlled, are listed in Tables 6 and 7. All the results are accord with the conclusion above but for Load case 1, the case 1 slight outperforms than case II in RMS responses.

3.4 Seismic response analysis

The dynamic responses of jacket offshore platform-TID system subjected to four earthquakes are calculated and examined. First, the Hachinohe earthquake is considered and the displacement and absolute acceleration responses of deck level are shown as follows.

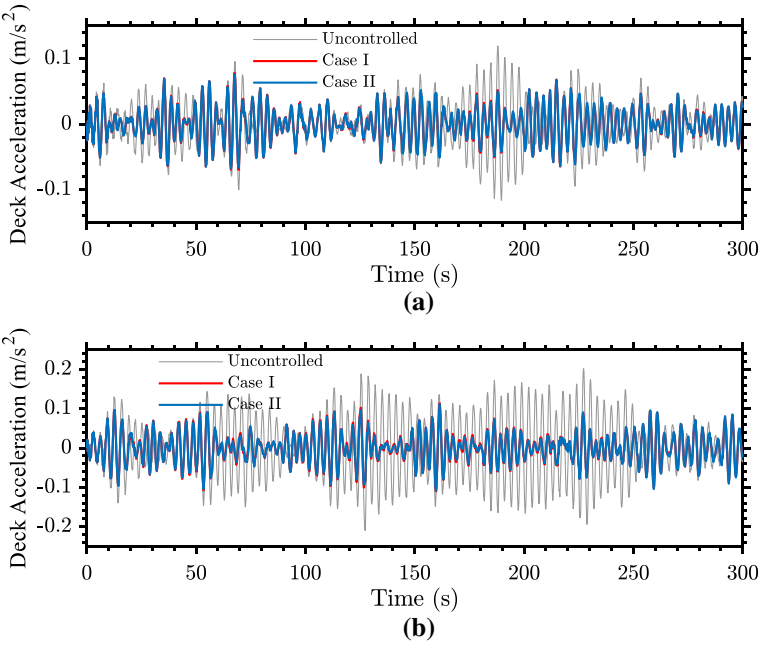

Fig. 7 Time history responses of jacket offshore platform deck acceleration considering two optimization cases of TID system and two wave load cases: **a** load case 1, **b** load case 2

Table 6 Deck displacements of jacket offshore platform with and without TID controlled

	Optimization	Index	Uncontrolled (m)	Controlled (m)	Reduction (%)
Load case 1	Case I	Maximum	0.0359	0.0278	22.63
		Minimum	−0.0333	−0.0240	29.11
		RMS	0.0109	0.0087	19.94
	Case II	Maximum	0.0359	0.0270	24.92
		Minimum	−0.0333	−0.0233	30.04
		RMS	0.0109	0.0088	19.41
Load case 2	Case I	Maximum	0.0792	0.0497	37.19
		Minimum	−0.0673	−0.0367	45.44
		RMS	0.0224	0.0134	40.33
	Case II	Maximum	0.0792	0.0484	38.91
		Minimum	−0.0673	−0.0368	45.32
		RMS	0.0224	0.0133	40.54

Table 7 Deck accelerations of jacket offshore platform with and without TID controlled

	Optimization	Index	Uncontrolled (m/s^2)	Controlled (m/s^2)	Reduction (%)
Load case 1	Case I	Maximum	0.1195	0.0785	34.29
		Minimum	−0.1162	−0.0697	39.98
		RMS	0.0349	0.0247	29.18
	Case II	Maximum	0.1195	0.0762	36.24
		Minimum	−0.1162	−0.0678	41.59
		RMS	0.0349	0.0249	28.78
Load case 2	Case I	Maximum	0.2023	0.1139	43.71
		Minimum	−0.2098	−0.1104	47.39
		RMS	0.0784	0.0377	51.99
	Case II	Maximum	0.2023	0.1117	44.78
		Minimum	−0.2098	−0.1082	48.44
		RMS	0.0784	0.0371	52.71

The time history of displacement relative to seabed and absolute acceleration of deck level are shown in Fig. 8a, b, respectively. The responses for two optimization cases of TID are also close to each other and the peak response of case I is slightly smaller than that of case II. The detailed maximum, minimum and RMS responses are calculated and listed in Table 8. The average reduction ratio in terms of case I and case II on maximum, minimum and RMS of deck relative displacement and absolute acceleration are 28.84%, 26.64% and 46.59%. Those reductions for deck absolute acceleration are 25.16%, 19.72% and 43.33%. These results verify the effect of TID on seismic response control for jacket offshore platform.

The seismic responses of the jacket offshore platform subjected to other three earthquakes are also evaluated. Figure 9 shows the time history of displacement relative to seabed and absolute acceleration of deck level when the jacket offshore platform is subjected to Hachinohe, Northridge, and Kobe earthquakes. The results are similar with

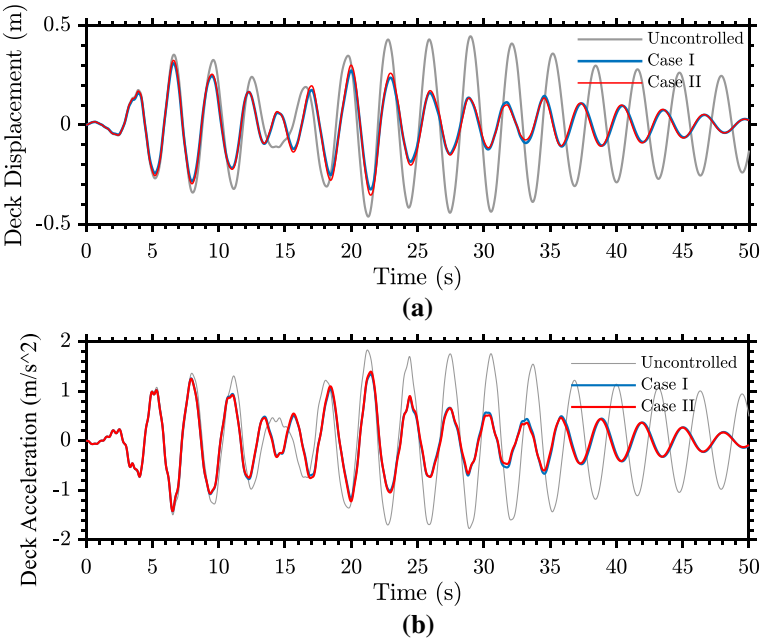

Fig. 8 Time history responses of jacket offshore platform considering two optimization cases of TID system. **a** deck displacement relative to seabed, **b** deck absolute acceleration

Table 8 Deck displacements and accelerations of jacket offshore platform with and without TID controlled

Response Type	Optimization	Index	Uncontrolled (morm/s^2)	Controlled (morm/s^2)	Reduction (%)
Displacement	Case I	Maximum	0.44628	0.31019	30.4943
		Minimum	−0.46163	−0.32409	29.7943
		RMS	0.22848	0.11868	48.057
	Case II	Maximum	0.44628	0.32491	27.195
		Minimum	−0.46163	−0.3532	23.4897
		RMS	0.22848	0.12539	45.1185
Acceleration	Case I	Maximum	1.8328	1.3472	26.4946
		Minimum	−1.7685	−1.4221	19.5856
		RMS	0.90431	0.51232	43.3468
	Case II	Maximum	1.8328	1.3962	23.82
		Minimum	−1.7685	−1.4175	19.8477
		RMS	0.90431	0.51267	43.3085

that when the excitation is Hachinohe earthquake, i.e., the TID with optimization case I outperform slightly that case II on mitigation of peak responses. For optimization case I, the maximum displacement responses are reduced as 46.95%, 44.25%, and 19.94% for El Centro, Northridge, and Kobe earthquakes, respectively. While the reduction on

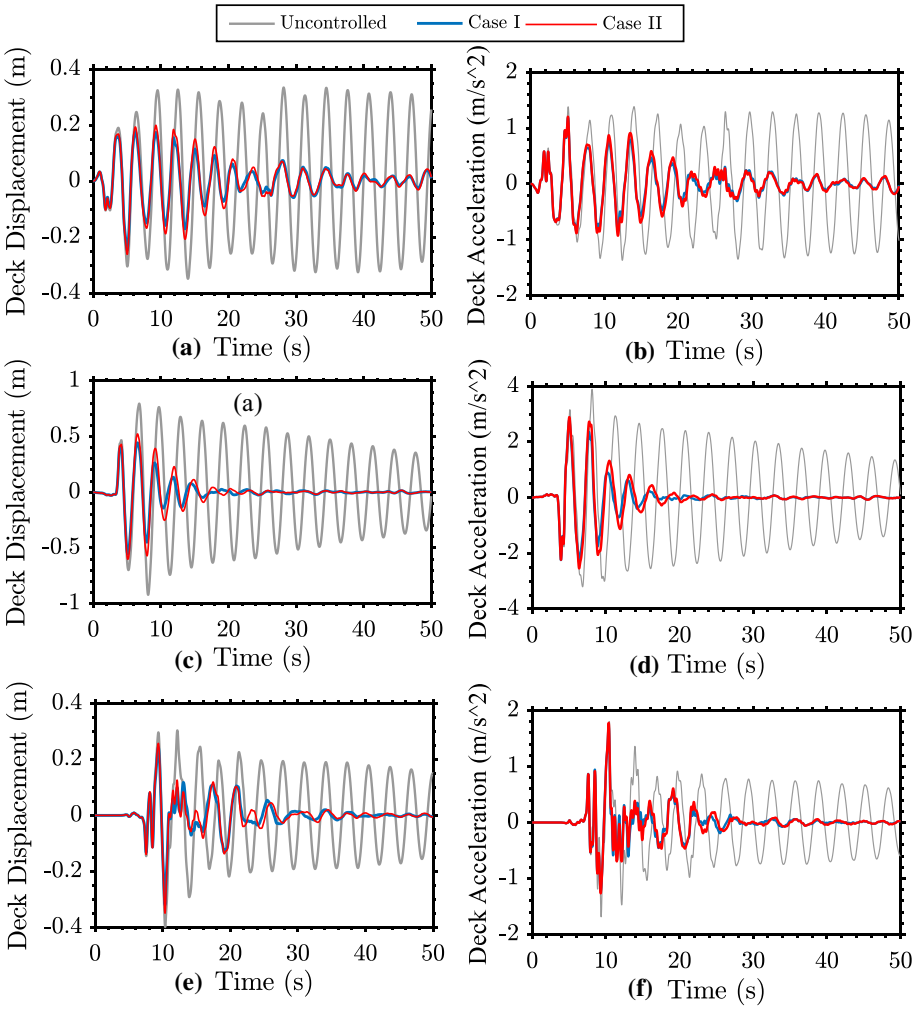

Fig. 9 Deck displacement and acceleration responses of jacket offshore platform considering two optimization cases of TID system. **a**, **b** El Centro earthquake; **c**, **d** Northridge earthquake; and **e**, **f** Kobe earthquake

maximum acceleration of offshore platform are 14.43%, 28.42%, and 4.74% for El Centro, Northridge, and Kobe earthquakes, respectively.

3.5 Comparison of different loadings

From above analysis it can be seen that the optimization case I and II of TID are much effective for earthquake load and wave load, respectively. Assuming $\tilde{y}_{\mathrm{I}}$ and $\tilde{y}_{\mathrm{II}}$ are the maximum deck displacements when platform is controlled by optimization case I and II of TID, respectively, then a simple performance index

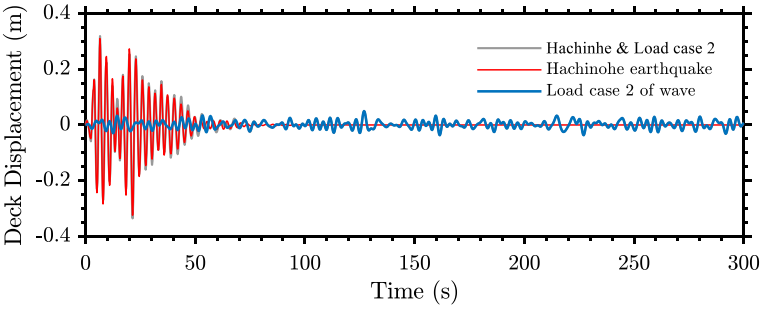

Fig. 10 Time history of deck displacement for different load and combination of loads

$$J_{\max} = \tilde{y}_{\mathrm{I}} - \tilde{y}_{\mathrm{II}} \tag{34}$$

is defined to evaluate the difference of two optimization cases when different loadings act on jacket offshore platform. If $J_{\max} > 0$, it denotes that optimization case II of TID is more appropriate for wave load, and vice versa. For example, for load case 2 of irregular wave loading, the $J_{\max}$ is 0.0014, while for earthquake load (considering the Hachinohe earthquake), the $J_{\max}$ is -0.0147. When the platform-TID system is subjected to Hachinohe signal and irregular wave loads, the deck displacements are shown in Fig. 10.

It can see that in Fig. 10 the response excited by earthquake dominates. Thus if the jacket offshore platform is excited by earthquake and wave simultaneously, the case II of TID is preferred. This is because the energy of earthquake is much larger than that of sea wave. For further analysis, the jacket offshore platform-TID system subjected to both Hachinohe signal load and load case 2 of wave load and the Hachinohe signal is scaled by $\eta \in [0 : 0.1 : 1]$, then the relation between $J_{\max}$ and η is examined.

As shown in Fig. 11, the index $J_{\max}$ decreases as the η increases from 0 to 1. The $J_{\max}$ approximately equal to zero when $\eta = 0.15$. This indicates that the case I is preferred when $\eta > 0.15$, otherwise case II outperforms that case I. The magnitude of 0.15 Hachinohe may be easy to achieve for earthquake but a wave with 100-year period is not often encountered in real-life. Thus the optimization design case I is attractive in term of cost-effectiveness if an offshore platform is located in a seismically active region.

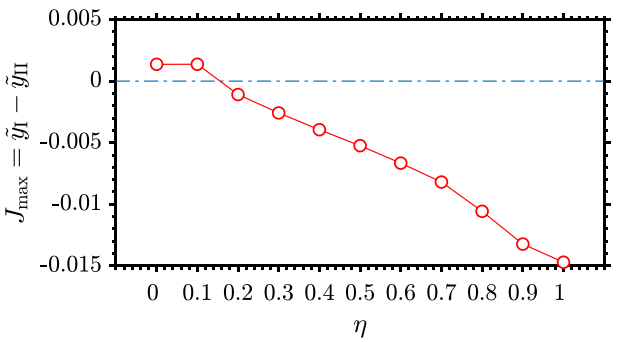

Fig. 11 The performance comparison of case I and case II when jacket offshore platform-TID system is excited by load case 2 of wave and scaled Hachinohe signal

4 Conclusion

This study proposes the adoption of TID system to control undesirable vibration of jacket offshore platforms subjected to wave and earthquake loads. Analytical models of the jacket platform equipped TID system with different action of excitations is developed. An analytical optimal design approach of TID which can be used for wave and earthquake load is proposed, and wave loadings under different sea states were calculated by Morrison equation.

The time history responses of the practical 90 (m) high jacket platform have verified the efficiency of TID system. From the case study, it reveals that the optimal installation location of TID for jacket offshore platforms subjected to wave or earthquake are both top level, i.e. the deck level. Signification reduction on responses of jacket platform is achieved by the use of TID. For example, for load case 2 of wave load, the reduction ratio in average values of the maximum, minimum and RMS of the deck displacement by TID system are 38.05%, 45.38%, and 40.435%, respectively. While for acceleration responses, the reduction ratio of that are 44.25%, 47.92%, and 52.35%. The results reveal that the TID is more effective for control of acceleration responses of platform and for harsher waves. The feasibility of TID system for control seismic responses of platform structures has been verified in the numerical example. When considering the Hachinohe earthquake as a representative, the average reduction ratio in terms of case I and case II on maximum, minimum and RMS of deck relative displacement are 28.84%, 26.64% and 46.59%. For deck absolute acceleration they are 25.16%, 19.72% and 43.33%, respectively. Finally, the comparison of multiple-hazard excitations reveal that the earthquake-induced responses are more drastic, and thereby the TID should is tuned according to earthquake case if the jacket offshore platforms is located at a seismic active region.

Funding Open Access funding enabled and organized by CAUL and its Member Institutions. The authors have not disclosed any funding.

Declaration

Competing Interests The authors declared that they have no conflicts of interest to this work.

References

Asami T, Wakasono T, Kameoka K, Hasegawa M, Sekiguchi H (1991) Optimum design of dynamic absorbers for a system subjected to random excitation*. JSME Int J 34(2):218–226

Bin W, Pengfei S, Qianying W, Xinchun G, Jinping O (2011) Performance of an offshore platform with MR dampers subjected to ice and earthquake. Struct Control Health Monit 18(6):682–697. https://doi.org/10.1002/stc

Chaiviriyawong P, Webster WC, Pinkaew T, Lukkunaprasit P (2007) Simulation of characteristics of tuned liquid column damper using a potential-flow method. Eng Struct 29(1):132–144. https://doi.org/10.1016/j.engstruct.2006.04.021

Das D, Khan M (2020) Hybrid control of offshore jacket platforms using decentralized sliding mode control and shape memory alloy-rubber bearing under multiple hazards. J Offshore Mech Arct Eng **142**(1):1. https://doi.org/10.1115/1.4044361.

De Domenico D, Ricciardi G (2018a) An enhanced base isolation system equipped with optimal tuned mass damper inerter (TMDI). Earthq Eng Struct Dynam 47(5):1169–1192. https://doi.org/10.1002/eqe.3011

De Domenico D, Ricciardi G (2018b) Optimal design and seismic performance of tuned mass damper inerter (TMDI) for structures with nonlinear base isolation systems. Earthq Eng Struct Dyn 47(12):2539–2560. https://doi.org/10.1002/eqe.3098

De Angelis M, Giaralis A, Petrini F, Pietrosanti D (2019) Optimal tuning and assessment of inertial dampers with grounded inerter for vibration control of seismically excited base-isolated systems. Eng Struct 196:109250. https://doi.org/10.1016/j.engstruct.2019.05.091

De Angelis M, Petrini F, Pietrosanti D (2021) Optimal design of the ideal grounded tuned mass damper inerter for comfort performances improvement in footbridges with practical implementation considerations. Struct Control Health Monit 28(9):1–26. https://doi.org/10.1002/stc.2800

Di Matteo A, Masnata C, Pirrotta A (2019) Simplified analytical solution for the optimal design of Tuned Mass Damper Inerter for base isolated structures. Mech Syst Signal Process 134:106337. https://doi.org/10.1016/j.ymssp.2019.106337

Enferadi MH, Ghasemi MR, Shabakhty N (2019) Wave-induced vibration control of offshore jacket platforms through SMA dampers. Appl Ocean Res 90:101848. https://doi.org/10.1016/j.apor.2019.06.005

Ghasemi MR, Shabakhty N, Enferadi MH (2019) Vibration control of offshore jacket platforms through shape memory alloy pounding tuned mass damper (SMA-PTMD). Ocean Eng 191:106348. https://doi.org/10.1016/j.oceaneng.2019.106348

Giaralis A, Petrini F (2017) Wind-induced vibration mitigation in tall buildings using the tuned mass-damper-inerter. J Struct Eng (US) 143(9):1–11. https://doi.org/10.1061/(ASCE)ST.1943-541X.0001863

Goda Y (1970) Numerical Simulation of Ocean Waves for Statistical. Analysis 33(3):5–14

Gonzalez-Buelga A, Lazar IF, Jiang JZ, Neild SA, Inman DJ (2017) Assessing the effect of nonlinearities on the performance of a tuned inerter damper. Struct Control Health Monit 24(3):e1879. https://doi.org/10.1002/stc

Hasselmann K, Barnett TP, Bouws E, Carlson H, Cartwright DE, Eake K, et al (1973) Measurements of wind-wave growth and swell decay during the joint North Sea wave project (JONSWAP). Ergänzungsheft Zur Deutschen Hydrographischen Zeitschrift, Reihe A, Nr 12

Hirdaris SE, Bai W, Dessi D, Ergin A, Gu X, Hermundstad OA et al (2014) Loads for use in the design of ships and offshore structures. Ocean Eng 78:131–174. https://doi.org/10.1016/j.oceaneng.2013.09.012

Hokmabady H, Mojtahedi A, Mohammadyzadeh S, Ettefagh MM (2019a) Structural control of a fixed offshore structure using a new developed tuned liquid column ball gas damper (TLCBGD). Ocean Eng 192:106551. https://doi.org/10.1016/j.oceaneng.2019.106551

Hokmabady H, Mohammadyzadeh S, Mojtahedi A (2019b) Suppressing structural vibration of a jacket-type platform employing a novel Magneto-Rheological Tuned Liquid Column Gas Damper (MR-TLCGD). Ocean Eng 180:60–70. https://doi.org/10.1016/j.oceaneng.2019.03.055

Hu Y, Chen MZQ (2015) Performance evaluation for inerter-based dynamic vibration absorbers. Int J Mech Sci 99:297–307. https://doi.org/10.1016/j.ijmecsci.2015.06.003

Hu Y, Chen MZQ, Shu Z, Huang L (2015) Analysis and optimisation for inerter-based isolators via fixed-point theory and algebraic solution. J Sound Vib 346(1):17–36. https://doi.org/10.1016/j.jsv.2015.02.041

Hu Y, Wang J, Chen MZQ, Li Z, Sun Y (2018) Load mitigation for a barge-type floating offshore wind turbine via inerter-based passive structural control. Eng Struct 177:198–209. https://doi.org/10.1016/j.engstruct.2018.09.063

Ikago K, Saito K, Norio I (2012) Seismic control of single-degree-of-freedom structure using tuned viscous mass damper. Earthq Eng Struct Dynam 41(3):453–474. https://doi.org/10.1002/eqe.1138

Ikago K, Sugimura Y, Saito K, Inoue N (2011) Seismic displacement control of multiple-degree-of-freedom structures using tuned viscous mass dampers. In: Proceedings of the 8th international conference on structural dynamics, EURODYN 2011 2011 1(3)1800–1807

Jin Q, Li X, Sun N, Zhou J, Guan J (2007) Experimental and numerical study on tuned liquid dampers for controlling earthquake response of jacket offshore platform. Mar Struct 20(4):238–254. https://doi.org/10.1016/j.marstruc.2007.05.002

Lazar IF, Neild SA, Wagg DJ (2014) Using an inerter-based device for structural vibration suppression. Earthq Eng Struct Dyn 43(8):1129–1147
Lazar IF, Neild SA, Wagg DJ (2016) Vibration suppression of cables using tuned inerter dampers. Eng Struct 122:62–71. https://doi.org/10.1016/j.engstruct.2016.04.017
Lee HH (1997) Stochastic analysis for offshore structures with added mechanical dampers. Ocean Eng 24(9):817–834. https://doi.org/10.1016/s0029-8018(96)00039-x
Leng D, Zhu Z, Xu K, Li Y, Liu G (2021) Vibration control of jacket offshore platform through magnetorheological elastomer (MRE) based isolation system. Appl Ocean Res 114:102779. https://doi.org/10.1016/j.apor.2021.102779
Liu X, Li G, Yue Q, Oberlies R (2009) Acceleration-oriented design optimization of ice-resistant jacket platforms in the Bohai Gulf. Ocean Eng 36(17–18):1295–1302. https://doi.org/10.1016/j.oceaneng.2009.09.008
Ma R, Bi K, Hao H (2018) Mitigation of heave response of semi-submersible platform (SSP) using tuned heave plate inerter (THPI). Eng Struct 177:357–373. https://doi.org/10.1016/j.engstruct.2018.09.085
Ma R, Bi K, Hao H (2019) A novel rotational inertia damper for heave motion suppression of semisubmersible platform in the shallow sea. Struct Control Health Monit 26(7):1–24. https://doi.org/10.1002/stc.2368
Ma R, Bi K, Hao H (2020) Using inerter-based control device to mitigate heave and pitch motions of semi-submersible platform in the shallow sea. Eng Struct 207:110248. https://doi.org/10.1016/j.engstruct.2020.110248
Ma R, Bi K, Hao H (2021) Inerter-based structural vibration control: a state-of-the-art review. Eng Struct 243:112655. https://doi.org/10.1016/j.engstruct.2021.112655
Marian L, Giaralis A (2014) Optimal design of a novel tuned mass-damper-inerter (TMDI) passive vibration control configuration for stochastically support-excited structural systems. Probab Eng Mech 38:156–164. https://doi.org/10.1016/j.probengmech.2014.03.007
Ou J, Long X, Li QS, Xiao YQ (2007) Vibration control of steel jacket offshore platform structures with damping isolation systems. Eng Struct 29(7):1525–1538. https://doi.org/10.1016/j.engstruct.2006.08.026
Patil KC, Jangid RS (2005) Passive control of offshore jacket platforms. Ocean Eng 32(16):1933–1949. https://doi.org/10.1016/j.oceaneng.2005.01.002
Pietrosanti D, De Angelis M, Basili M (2017) Optimal design and performance evaluation of systems with Tuned Mass Damper Inerter (TMDI). Earthq Eng Struct Dyn 46(8):1367–1388. https://doi.org/10.1002/eqe.2861
Pourzangbar A, Vaezi M (2021) Optimal design of brace-viscous damper and pendulum tuned mass damper using Particle Swarm Optimization. Appl Ocean Res 112:102706. https://doi.org/10.1016/j.apor.2021.102706
Pourzangbar A, Vaezi M, Mousavi SM, Saber A (2020) Effects of brace-viscous damper system on the dynamic response of steel frames. Int J Eng Trans B 33(5):720–731. https://doi.org/10.5829/IJE.2020.33.05B.02
Shen W, Niyitangamahoro A, Feng Z, Zhu H (2019) Tuned inerter dampers for civil structures subjected to earthquake ground motions: optimum design and seismic performance. Eng Struct 198:109470. https://doi.org/10.1016/j.engstruct.2019.109470
Smith MC (2002) Synthesis of mechanical networks: The inerter J. IEEE Trans Autom Control 47(10):1648–1662. https://doi.org/10.1109/TAC.2002.803532
Suhardjo J, Kareem A (2001) Feedback–feedforward control of offshore platforms under random waves. Earthq Eng Struct Dynam 30(2):213–235. https://doi.org/10.1002/1096-9845(200102)30:2%3c213::aid-eqe5%3e3.3.co;2-w
Sun L, Hong D, Chen L (2017) Cables interconnected with tuned inerter damper for vibration mitigation. Eng Struct 151:57–67. https://doi.org/10.1016/j.engstruct.2017.08.009
Vaezi M, Pourzangbar A, Fadavi M, Mousavi SM, Sabbahfar P, Brocchini M (2021) Effects of stiffness and configuration of brace-viscous damper systems on the response mitigation of offshore jacket platforms. Appl Ocean Res 107:102482. https://doi.org/10.1016/j.apor.2020.102482
Xu K, Bi K, Han Q, Li X, Du X (2019) Using tuned mass damper inerter to mitigate vortex-induced vibration of long-span bridges: analytical study. Eng Struct 182:101–111. https://doi.org/10.1016/j.engstruct.2018.12.067
Xu T, Li Y, Lai T, Zheng J (2021) A simplified design method of tuned inerter damper for damped civil structures: Theory, validation, and application. Struct Control Health Monit 28(9):e2789. https://doi.org/10.1002/stc.2798
Xu T, Yang G, Li Y, Lai T. Influence of inerter-based damper installations on control efficiency of building structures. Struct Control Health Monit 2022:e2929. https://doi.org/10.1002/stc.2929.

Yue Q, Zhang L, Zhang W, Kärnä T (2009) Mitigating ice-induced jacket platform vibrations utilizing a TMD system. Cold Reg Sci Technol 56(2–3):84–89. https://doi.org/10.1016/j.coldregions.2008.11.005
Zhang BL, Han QL, Zhang XM (2017) Recent advances in vibration control of offshore platforms. Nonlinear Dyn 89(2):755–771. https://doi.org/10.1007/s11071-017-3503-4